Journal of
Materials Chemistry C

Accepted Manuscript

Structure and composition characterization of lead-free (K, Na)NbO_3 piezoelectric nanorods synthesized by molten-salt reaction

Composition-controlled (K, Na)NbO_3 piezoelectric nanorods were synthesized, and the chemical homogeneity and Raman frequency dependence on alkaline contents were investigated.

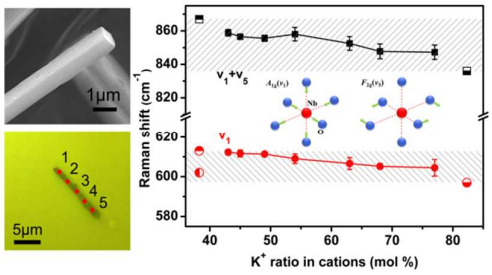

Journal of
Materials Chemistry C

RSCPublishing

ARTICLE

Structure and composition characterization of lead-free (K, Na)NbO_3 piezoelectric nanorods synthesized by molten-salt reaction

Li-Qian Cheng, Ke Wang, Qi Yu and Jing-Feng Li*

Cite this: DOI: 10.1039/x0xx00000x

Received ooth January 2012,
Accepted ooth January 2012

DOI: 10.1039/x0xx00000x

www.rsc.org/

Lead-free (K,Na)NbO_3 single crystalline nanorods (KNN NRs) with environmental compatibility and high piezoelectric coefficient may find increasing applications including piezoelectric nanogenerators. To optimize the piezoelectric responses of KNN NRs, the K/Na ratio must be adjusted precisely to a critical value. In this work, composition-controlled KNN NRs were successfully synthesized via molten-salt reaction, and some advanced measuring techniques, such as Raman, ICP, TEM, DSC, *etc.*, were employed for the detailed characterization. The compositional homogeneity along the length direction of an individual NR was confirmed by confocal Raman spectroscopy. Furthermore, this work revealed the correlation between the characteristic frequencies of Raman spectra and K/Na ratio of KNN nanocrystals, which can be used as a simple and convenient method for non-destructive and quantitative analysis of the A-site composition in alkaline niobate perovskite compounds.

1 Introduction

Piezoelectric materials in the nanostructured forms have attracted extensive attention as a result of their interesting size-dependent properties and promising applications.[1, 2] Specifically, the 1-D structures, such as nanorods,[3] nanowires,[4-6] nanotubes[7] and nanobelts,[8, 9] have been expected to play an important role as functional and interconnection units at the nanoscale.[1] Nano-sized piezoelectrics and their derivative composites with other components, such as polymers possess advantages of intriguing flexibility and adoptability, which is essential for future technology tendency. From the viewpoint of materials development, the implementation goes from simple binary compounds to complex compositions, which may meet more difficulties about their synthesis but could provide superior performance.[1] For instance, ZnO nanorods/nanowires have been firstly developed as mechanical-electrical triggers and sensors,[10] demonstrating impressive advantages of combining piezoelectric oxides and nanotechnology, even though the piezoelectric constant d_{33} of ZnO is as low as around 10 pC/N. Recent interests have been focused on the nanostructures of perovskite oxides with salient ferroelectric/piezoelectric properties, such as $BaTiO_3$,[11-15] Pb(Zr, Ti)O_3 (PZT),[16, 17] (K, Na)NbO_3 (KNN),[18-20] and so on,[21] which possess a large d_{33} of 100-600 pC/N. These 1-D perovskite structures could be more efficiently integrated in various devices, such as energy-harvesters, in which they can serve as voltage generators to convert mechanical input into electrical power directly.[22] Alternatively, their large dielectric permittivity leads to promising applications as capacitor components in flexible and portable devices.[23]

Recently, the lead-free (K, Na)NbO_3 (abbreviated as KNN)-based system has received much attention due to the increasing environmental concern as well as its uncovered outstanding properties, such as considerable d_{33} of 300-400 pC/N, high Cuire temperature (T_C) beyond 400 ℃, *etc.*.[24-26] The KNN materials are expected as promising alternatives to substitute for currently market-dominating PZT ceramics, which contain over 60 wt% lead and are thus ineluctably toxic. Certainly, the advantages of KNN systems have stimulated the studies of KNN-based nanomaterials. Actually, recent reports exhibit that 1-D KNN nanostructures have been successfully synthesized by molten salt and hydrothermal routes.[1, 27, 28]

Compared to ZnO, KNN shows much more complexity in compositions, which inevitably leads to challenges during synthesis procedures. Moreover, it is generally accepted that the ferroelectric and piezoelectric properties of KNN materials can be tailored by the K/Na ratio, while those containing nearly equal amount of Na and K elements are expected to demonstrate the optimal piezoelectric output.[26, 29] However, it would be a challenge for synthesizing KNN materials with controlled compositions at the nano- or micro-scale. For instance, the K/Na ratio normally deviates from the nominal compositions of starting powders in hydrothermal process.[30] Xu *et al.* also reported the deviated composition results during the fabrication of KNN nanorods aligned on the STO/KNN ($SrTiO_3$/KNN) substrate.[18] Besides, it must be stressed that the content of light elements such as Na and K are not easily determined by general facilities, e.g. Energy Dispersive

Spectrometer (EDS) or X-ray Fluorescence (XRF), which brings additional difficulty to this issue.

In the current study, composition-controlled KNN NRs were successfully synthesized by the molten-salt reaction, while the A-site K/Na ratio is adjusted by ratios of K_2CO_3/Na_2CO_3 in the KCl salt. The compositions of KNN NRs, together with crystal structures, were elaborately examined by inductively coupled plasma spectroscopy (ICP) and X-ray diffraction (XRD), respectively. In addition, the variation of K/Na in KNN NRs was further confirmed by DSC measurement. Most importantly, the dependence of Raman shifts on K/Na ratios in KNN NRs was elaborately established, which offered a convenient and accurate route for compositional determination in the current material system. Furthermore, KNN NRs with variable alkaline compositions are expected to be utilized to evaluate the relationship between piezoelectric properties and compositions, and promote the understanding on the phase structure in the KNN system.

2 Experimental

Synthesis of KNN NRs via molten-salt reaction

The KNN NRs products were synthesized according to a step-by-step procedure, which is mainly consisted of four steps. The detailed procedure could be found in a previous study.[19] Sodium carbonate (Na_2CO_3, 99.8 %, Sinopharm Chemical Reagent Co. (SCRC), Beijing, China), potassium carbonate (K_2CO_3, 99 %, SCRC), niobium oxide (Nb_2O_5, 99.95 %, Conghua Tantalum & Niobate Smeltery, Guangzhou, China) and KCl (99.5 %, SCRC, China) were used as raw materials. Firstly (Step 1), Nb_2O_5, K_2CO_3 and KCl were mixed in the presence of ethanol and milled for 1h in an Y_2O_3-stablized ZrO_2 (YTZ) ceramic jar. The mixture was dried and heated up to 1000 ℃ and held for 3 h, followed by washing the products of Step 1, *i.e.* $K_6Nb_{10.8}O_{30}$ NRs, with hot deionized water to remove the excessive KCl. Secondly (Step 2), the dried $K_6Nb_{10.8}O_{30}$ NRs were stirred in $HNbO_3$ solution for 48 h at room temperature, and washed for several times to keep the products neutral. Thirdly (Step 3), the products obtained in Step 2 were soaked at 550 ℃ for 1 h to achieve Nb_2O_5 NRs. Finally (Step 4), Nb_2O_5 NRs were mixed with different K_2CO_3/Na_2CO_3 ratios in KCl salt. Subsequently, the mixture were washed again with hot deionized water and dried, and (K, Na)NbO_3 NRs were obtained.

Characterization of KNN NRs

The crystal structure of the products from each reaction step was determined by X-ray diffraction (XRD, Rigaku, D/Max2500, Japan) using CuKα radiation (λ = 1.5406 Å). The morphology of the synthesized products was observed by scanning electron microscopy (SEM, JEOL JSM-7001F, Japan). The microstructure of the products was analyzed by transmission electron microscopy (TEM, Tecnai G20, FEI, USA). After completely dissolving the KNN NRs of ~100 mg in the mixture of HF and H_2SO_4 acid, the weight percent of alkaline elements was determined using inductively coupled plasma spectroscopy (ICP-AES, Varuan, Vista-MPX, USA) instrument, and the molar ratio of K/Na could be calculated from the obtained data. The phase structure and the composition of the products were examined by Raman spectrum (LabRAM HR, HORIBA Jobin Yvon, France) with an excitation wavelength of 488 nm. The phase transition temperatures of KNN NRs were evaluated by differential scanning calorimetry (DSC, STA 449 F3, Netzsch, Germany) analysis. In addition, the possible existence of residual KCl was eliminated by X-ray fluorescence spectrometer (XRF-1800, Shimadzu, Sequential, Japan).

3 Results and discussions

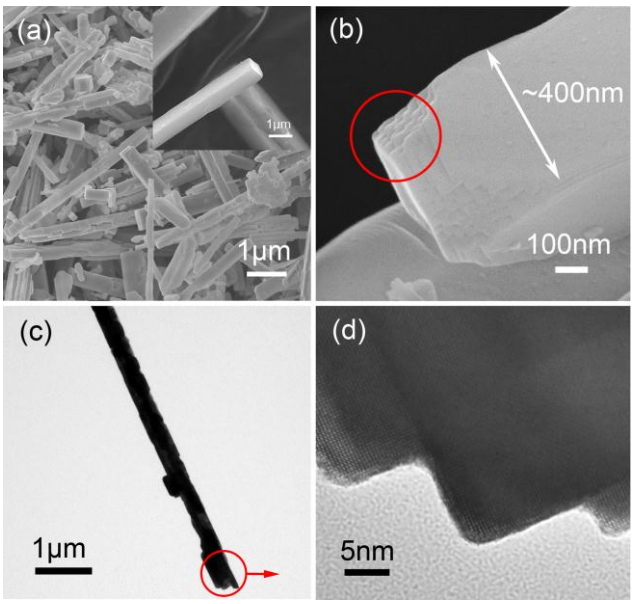

Fig. 1 (a) SEM images of the KNN NRs and the top view of an individual KNN NR showing the square cross section, (b) the nano-scaled crystal growth steps at the tip of a representative NR, (c) TEM image of an individual NR, and (d) HRTEM images of selected area with circular frame in (c).

Figure 1 shows the SEM/TEM results of the representative KNN NRs synthesized in the final step (Step 4). The observation of final products shown in Fig. 1(a) revealed that the diameters of the KNN NRs ranged from ~200 nm to ~700 nm, while whose lengths decreased to 10-20 micrometers perhaps due to the slight dissolution of Nb_2O_5 NRs in the molten salt.[13, 31] The top-view shown in Fig. 1(a) was almost of square shape. At the tip of an individual NR, the nano-scaled steps were observed, as marked with the red circle in Fig. 1(b), which corresponds to the growth stages of KNN NRs.[32] Thus, it seems that the preferential growth direction of KNN NRs is along the length orientation. TEM images of a representative KNN NR with 40 mol% K_2CO_3 in carbonates were also presented in Fig. 1(c). Single crystalline nature of KNN NRs was confirmed in the previous work,[19] and the unit cell parameters obtained in the high resolution TEM (HRTEM) image in Fig. 1(d) for KNN were determined to be 4.01 Å and 3.95 Å, corresponding to the <100> and <010> directions,

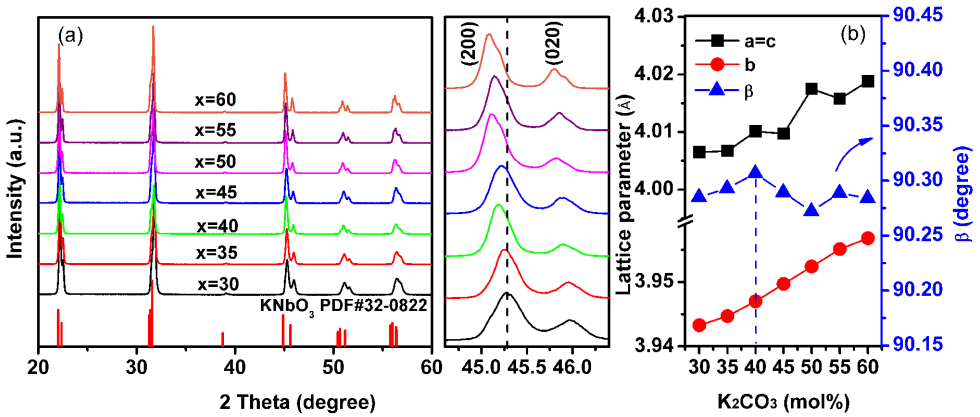

Fig. 2 (a) XRD patterns and enlarged peaks of (200) and (020) of the KNN NRs with K_2CO_3 in carbonate reactants (x mol%) are 30, 35, 40, 45, 50, 55 and 60, respectively, and (b) lattice parameters and β of all the corresponding products.

respectively. These values are in accordance with the calculated lattice parameters based on the XRD patterns in Fig. 2, and are also consistent with those of KNN bulk materials when the K/Na ratio is ~50/50.[33, 34] As shown in Fig. 1(b), the nano-sized steps at the tip of the NR were observed, and the TEM images in Fig. 1(d) further confirmed the stepped morphologies. The nano-sized steps at a corner of the NR end, whose heights were ~5-10 nm, providing the evidence of growth mechanism with preferential orientations.[18, 28, 35]

The KNN NRs are synthesized as shown in Fig. 1, while the formation of NRs with the composition of $K_{0.5}Na_{0.5}NbO_3$ is assumed as depicted in the following reaction when x is 0.5,

$$Nb_2O_5 + xK_2CO_3 + (1-x)Na_2CO_3 \xrightarrow{KCl} 2K_xNa_{1-x}NbO_3 + CO_2\uparrow \quad (1)$$

K_2CO_3 and Na_2CO_3 serve as the reactants in the KCl molten salt. A variable, x, is used to define the molar ratio of K_2CO_3 in carbonates. Thus, the K/Na ratio could be controlled by modifying the value of x, while KNN NRs with K/Na ~1 are reasonably expected.

The phase structure of the KNN NRs was detected by XRD and shown in Fig. 2. All the KNN NRs with different x values ranging from 30 to 60 mol% shows matched patterns with that of $KNbO_3$, as indexed by PDF#32-0822 with an orthorhombic symmetry. No trace of any impurity phase is observed for all compositions. The enlarged (200) and (020) peaks trend to shift to lower angles due to increasing content of K^+ (1.64 Å), coordination number (CN)=12), which has larger cation radius as compared with that of Na^+ (1.39 Å, CN=12).[34, 36] The calculated lattice parameters, together with the β angle, are shown in Fig. 2(b). The values of a, b, c and β are calculated according to the profiles of the N=12 ({hkl}={222}) and N=16 ({hkl}=400) line groups.[33] The values of a and c are greater than that of b, and $\beta \neq 90^\circ$. The lattice parameters are increasing in proportion to the K_2CO_3 amount, which confirms the higher K content in KNN NRs.[29]

It is known that K/Na ratio control is critically important for achieving high piezoelectricity in KNN system, but the quantitative measurement of K and Na elements is not easy. ICP, a powerful tool for quantitatively determination of both heavy and light elements, was adopted in this work to determine ratios of K/Na in resultant KNN NRs. In addition, XRF was employed to confirm the absence of residual KCl in the resultant KNN NRs. As shown in Fig. 3, the K/Na ratio in the reactants in the molten salt. When K_2CO_3/Na_2CO_3 is set at 30/70, the K/Na content ratio in KNN NRs is ~43/57. With further increasing the K_2CO_3 amount in the reactant, the K content in KNN products continues to increase, and the content of K^+ reaches 77 % in cations when x is 60 mol%. The KNN NRs with nearly equal amount of K and Na are obtained when the x value is 40 mol%, as marked by the star- shaped symbol in the graph, which is derived from the expected K_2CO_3/Na_2CO_3 ratio of 50/50 as assumed in reaction (1). Therefore, it is clear that the K/Na ratios of resultants differ from those of starting materials. As long as the temperature rises up to the melting point of KCl salt, the salt transforms to the flux and acts as the solvent where Nb_2O_5, Na_2CO_3 and K_2CO_3 are solutes inside.[37] The KCl salt, which consists of K^+,

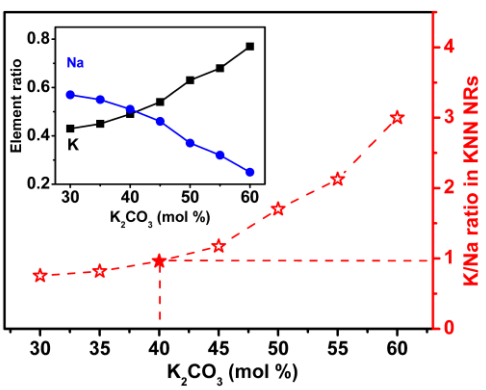

Fig. 3 The relative ratios of K and Na contents in KNN NRs detected by ICP, and the ratio is close to 1 (K/Na=~49/51) at K_2CO_3/Na_2CO_3 ~40/60.

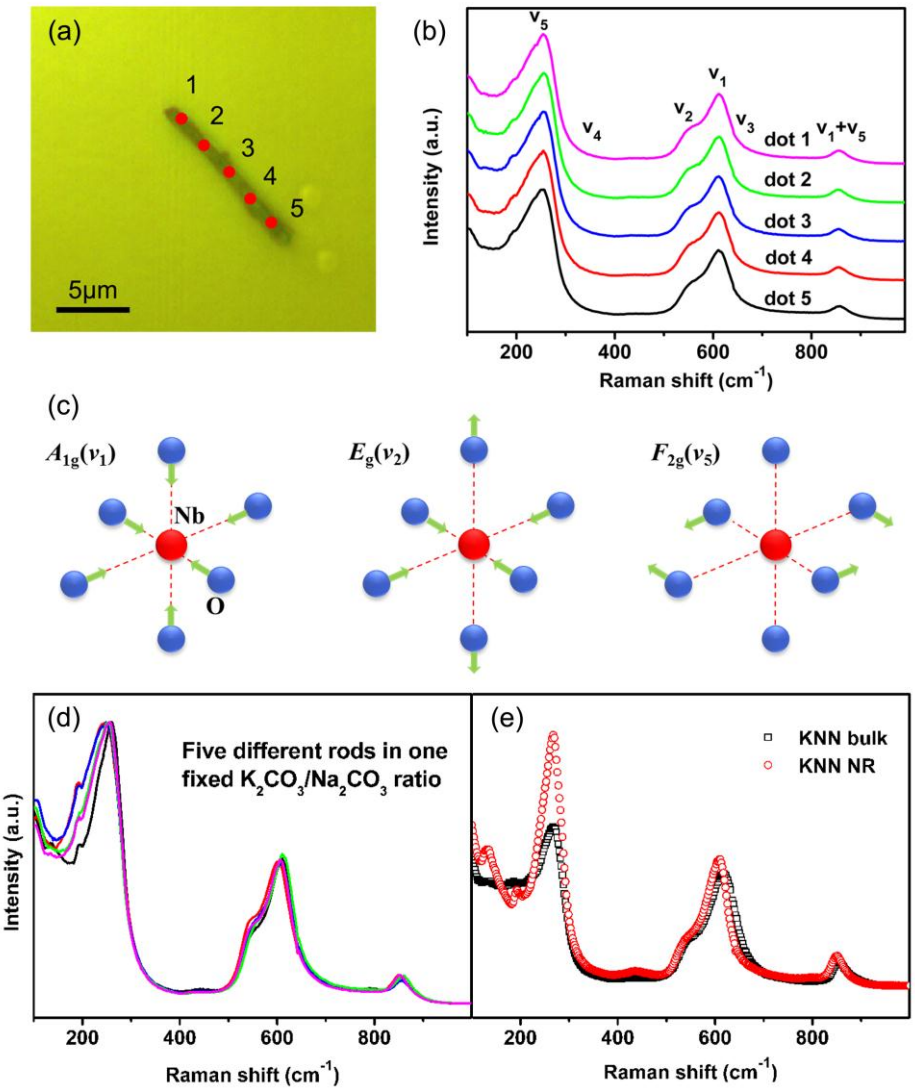

Fig. 4 (a) Selected five dot areas along the length direction of an individual NR, and (b) the corresponding Raman spectra of the five dots; (c) Schematic illustrations of three internal vibrational modes of NbO_6 octahedra, streching v_1 and v_2 modes, and bending v_5 mode, (d) Raman spectra of five different rods with the same K_2CO_3/Na_2CO_3 ratio as reactants, and (e) the comparison of spectra of KNN ($\sim K_{0.49}Na_{0.51}NbO_3$) NR and $K_{0.5}Na_{0.5}NbO_3$ bulk.

would not only serve as solvent but also participate in the reaction.[38] With further increasing temperature, the Na^+ from Na_2CO_3, and K^+ from K_2CO_3 as well as KCl would enter into the frame of Nb_2O_5. It seems that it is easy to obtain the KNN products with higher K concentration due to increased amount of K^+ sources from K_2CO_3 and KCl. On the other hand, Na^+ is easier to fill into the A site of the ABO_3 structure due to the smaller cation radius.[36] Our results show that, the K and Na cations would have the same probability to enter the A sites of ABO_3 structures when K_2CO_3 ratio is ~40 mol%; in other words, $K_{0.5}Na_{0.5}NbO_3$ NRs appears as the final product at this condition.

Compositional homogeneity is important for single crystals, but its analysis at the nanoscale is fairly difficult. In this work, it is expected that confocal Raman spectroscopy might be effective to check the compositional homogeneity along the length direction of KNN NRs. Noticeable variation of characteristic Raman scattering frequencies would be obtained if there are any compositional inhomogeneity and state change, which is mainly due to changes of K/Na ratios and the temperature change, respectively. The Raman spectra of KNN NRs measured at room temperature are shown in Fig. 4. The NRs were firstly dispersed in alcohol, and then the suspension was spread on a Pt-coated (thickness ~100 nm) silicon wafer substrate. The coated Pt layer did not affect the Raman scattering results of KNN NRs due to the absence of bond information for metals, and the focused spot was only ~1 μm in diameter. The temperature of the NR during Raman scattering

was not raised significantly, due to the low power (below 8 mW) of incident light and the high thermal conductivity of the Pt-coated Si wafer, which supported the KNN NRs. The Raman spectra from five selected areas along the length direction of one individual NR are shown in Fig. 4(b). Three kinds of internal vibrational modes of NbO_6 octahedra, *i.e.* v_1, v_2 and v_5, are schematically shown in Fig. 4(c). In particular, v_1 and v_5 modes which are detected as relatively strong signals, are visibly identified in the Raman spectra.[39] The spacing between each dot was set to ~5 μm, so the spectra presented the information of different parts along the NR. The spectra all possess typical peaks with almost identical Raman shifts,[40, 41] revealing high compositional uniformity along the length direction of the KNN NR. Nevertheless, there are minor deviations for compositions of different NRs from the same batch, as shown in Fig. 4(d). It may be attributed to the inhomogeneous distribution of reactants in the molten salt. Figure 4(e) compares the Raman scattering spectra of both KNN NRs and KNN bulk materials, the characteristic frequencies of which shows some distinction from each other. With the higher content of K, the measured v_1 mode of KNN bulk should be lower than that of $K_{0.49}Na_{0.51}NbO_3$ NRs theoretically.[42] However, the v_1 mode of KNN NRs has lower wavenumber perhaps due to the release of internal stress.[43]

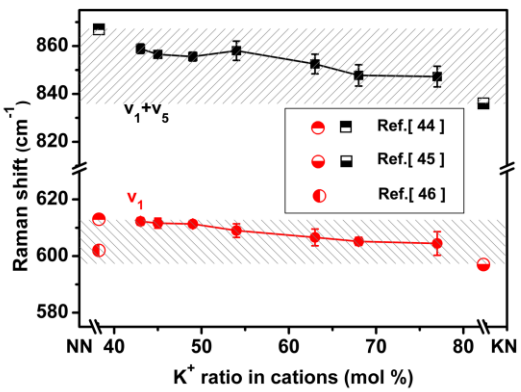

Fig. 5 Compositional dependence of Raman spectra for KNN single crystalline nanorod structure, and the six symbols marked in the graph stand for the references from the literatures.

In addition to the v_1 mode of KNN, the wavenumber corresponding to the coupling v_1+v_5 mode is found to change with the K/Na ratio. On the basis of ICP results, it is possible to create a compositional dependence of the Raman wavenumbers for the v_1 and v_1+v_5 modes as a function of K^+ content in the final KNN NRs. The frequencies of v_1 and v_1+v_5 modes of $KNbO_3$ (KN) and $NaNbO_3$ (NN) structures are also provided in the graph, respectively.[44-46] With the increasing amount of K_2CO_3 and resultant increasing K^+ content, these two modes shift to lower frequencies, which is in agreement with the frequency change from NN to KN. This result implies that there is a one-to-one correspondence between the feature frequencies of Raman spectra and the compositions of KNN single crystals. As a result, once the products are synthesized, the characteristic frequencies could be easily obtained by Raman scattering, which is a convenient and non-destructive approach, much easier than the ICP method. Accordingly, the compositions of the obtained KNN NR could be accurately identified from Fig. 5. This graph enables a facile way to determine the composition, especially the K/Na ratios of KNN materials using the non-destructive Raman spectra method, which certainly paves the way for the further investigations concerning fabrication of KNN NRs.

In order to further confirm the compositional variation of different KNN NRs, DSC measurement was utilized to check the phase transition temperatures, as shown in Fig. 6. Two endothermic peaks of the inset curve indicate the orthorhombic-tetragonal (T_{O-T}) and cubic-tetragonal transitions (Curie temperature, T_C), respectively. As shown in Fig. 6, T_C is roughly proportional to the increasing K^+ ratio in KNN NR, while the value of T_{O-T} minimizes at ~200 ℃ when K^+ equals ~49 mol%, which is in accordance with the phase diagram of KN-NN solid solution.[47] This result also confirms the compositional determination by ICP shown in Fig. 3.[48, 49] It is well-known that the movement of T_{O-T} toward room temperature would favor the enhancement of piezoelectricity.[34, 50] As a result, a high piezoresponse can be expected in the KNN NRs synthesized when K_2CO_3 ratio is controlled to ~40 mol%.

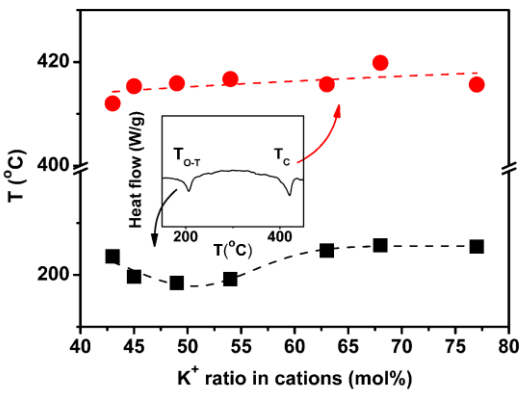

Fig. 6 DSC heating curves of KNN NRs which contain different K/Na ratios.

Conclusions

Nanostructured single crystalline KNN NRs with modified alkaline compositions were synthesized through the molten-salt reaction by adjusting the ratios of carbonates. As a result, the KNN NRs with an optimized K/Na ratio of approximately 1/1, which are expected to possess high piezoelectric response, were obtained when K_2CO_3/Na_2CO_3 reached at ~40/60. It is verified that an individual NR possessed a homogeneous K/Na distribution along the length direction. Furthermore, the compositional dependence of characteristic Raman shifts on K/Na ratio was finally depicted, which provides a simple and convenient way to characterize the A-site composition in KNN NRs. The ICP analysis, DSC measurement, together with XRD results all confirmed in the identification of K/Na ratios in the KNN NRs. The present study has established a facile and non-

destructive route for compositional determination of nano-sized structures, which would definitely enlighten further investigations.

Acknowledgements

This work is supported by the National Nature Science Foundation of China (Grants Nos. 51332002，51221291) and the Ministry of Science and Technology of China under the Grant 2009CB623304.

Notes and references

State Key Laboratory of New Ceramics and Fine Processing, School of Materials Science and Engineering, Tsinghua University, 100084, Beijing, P. R. China. E-mail: jingfeng@mail.tsinghua.edu.cn, Fax: +86-62771160; Tel: +86-10-62784845.

1 P. M. Rørvik, T. Grande and M.-A. Einarsrud, *Adv. Mater.*, 2011, **23**, 4007.
2 J. Varghese, R. W. Whatmore and J. D. Holmes, *J. Mater. Chem. C*, 2013, **1**, 2618.
3 J. J. Urban, W. S. Yun, Q. Gu and H. Park, *J. Am. Chem. Soc.*, 2002, **124**, 1186.
4 Y. Qin, X. Wang and Z. L. Wang, *Nature*, 2008, **451**, 809.
5 Y. Nakayama, P. J. Pauzauskie, A. Radenovic, R. M. Onorato, R. J. Saykally, J. Liphardt and P. Yang, *Nature*, 2007, **447**, 1098.
6 X. Li, Z. Dong, A. Westwood, A. Brown, R. Brydson, A. Walton, G. Yuan, Z. Cui and Y. Cong, *Cryst. Growth Des.*, 2011, **11**, 3122.
7 T.-J. Park, Y. Mao and S. S. Wong, *Chem. Commun.*, 2004, **23**, 2708.
8 Y. Yang, J. Qi, Y. Gu, W. Guo and Y. Zhang, *Appl. Phys. Lett.*, 2010, **96**, 123103.
9 J. Yu, S. Tang, R. Wang, Y. Shi, B. Nie, L. Zhai, X. Zhang and Y. Du, *Cryst. Growth Des.*, 2008, **8**, 1481.
10 J. Zhou, P. Fei, Y. Gao, Y. Gu, J. Liu, G. Bao and Z. L. Wang, *Nano Lett.*, 2008, **8**, 2725.
11 S. J. Limmer, S. Seraji, Y. Wu, T. P. Chou, C. Nguyen and G. Cao, *Adv. Funct. Mater.*, 2002, **12**, 59.
12 Y. Li, X. P. Gao, G. R. Li, G. L. Pan, T. Y. Yan and H. Y. Zhu, *J. Phys. Chem. C*, 2009, **113**, 4386.
13 K.-C. Huang, T.-C. Huang and W.-F. Hsieh, *Inorg. Chem.*, 2009, **48**, 9180.
14 N. P. Padture and X. Wei, *J. Am. Chem. Soc.*, 2003, **86**, 2215.
15 S. Hirano, S. Shimada and M. Kuwabara, *Appl. Phys. A*, 2005, **80**, 783.
16 S. Kawasaki, G. Catalan, H. J. Fan, M. M. Saad, J. M. Gregg, M. A. Correa-Duarte, J. Rybczynski, F. D. Morrison, T. Tatsuta, O. Tsuji and J. F. Scott, *Appl. Phys. Lett.*, 2008, **92**, 053109.
17 A. Nourmohammadi, M. A. Bahrevar, S. Schulze and M. Hietschold, *J.Mater. Sci.*, 2008, **43**, 4753.
18 Y. Xu, Q. Yu and J.-F. Li, *J. Mater. Chem.*, 2012, **22**, 23221.
19 L.-Q. Cheng, K. Wang and J.-F. Li, *Chem. Commun.*, 2013, **49**, 4003.
20 L. Li, J. Deng, R. Yu, J. Chen, X. Wang and X. Xing, *Inorg. Chem.*, 2010, **49**, 1397.
21 G. Suyal, E. Colla, R. Gysel, M. Cantoni and N. Setter, *Nano Lett.*, 2004, **4**, 1339.
22 Z. Wang, J. Hu, A. P. Suryavanshi, K. Yum and M.-F. Yu, *Nano Lett.*, 2007, **7**, 2966.
23 Y. Song, Y. Shen, P. Hu, Y. Lin, M. Li and C. W. Nan, *Appl. Phys. Lett.*, 2012, **101**, 152904.
24 Y. Saito, H. Takao, T. Tani, T. Nonoyama, K. Takatori, T. Homma, T. Nagaya and M. Nakamura, *Nature*, 2004, **432**, 84.
25 K. Wang and J.-F. Li, *Adv. Funct. Mater.*, 2010, **20**, 1924.
26 T. R. Shrout and S. Zhang, *J. Electroceram.*, 2007, **19**, 113.
27 C. Sun, X. Xing, J. Chen, J. Deng, L. Li, R. Yu, L. Qiao and G. Liu, *Eur. J. Inorg. Chem.*, 2007, **13**, 1884.
28 Z. Wang, H. Gu, Y. Hu, K. Yang, M. Hu, D. Zhou and J. Guan, *CrystEngComm*, 2010, **12**, 3157.
29 B.-P. Zhang, J.-F. Li, K. Wang and H. Zhang, *J. Am. Chem. Soc.*, 2006, **89**, 1605.
30 N. Liu, K. Wang, J.-F. Li and Z. Liu, *J. Am. Chem. Soc.*, 2009, **92**, 1884.
31 C.-Y. Xu, Q. Zhang, H. Zhang, L. Zhen, J. Tang and L.-C. Qin, *J. Am. Chem. Soc.*, 2005, **127**, 11584.
32 E. Vasco, A. Magrez, L. Forró and N. Setter, *J. Phys. Chem. B*, 2005, **109**, 14331.
33 K. Wang and J.-F. Li, *Appl. Phys. Lett.*, 2007, **91**, 262902.
34 Y.-J. Dai, X.-W. Zhang and K.-P. Chen, *Appl. Phys. Lett.*, 2009, **94**.
35 F. Madaro, J. R. Tolchard, Y. Yu, M.-A. Einarsrud and T. Grande, *CrystEngComm*, 2011, **13**, 1350.
36 R. D. Shannon, *Acta Cryst.*, 1976, **32**, 751.
37 K. H. Yoon, Y. S. Cho and D. H. Kang, *J. Mater. Sci.*, 1998, **33**, 2977.
38 L. Li, J. Chen, A. Deng, R. Yu, L. Qiao, G. Liu and X. Xing, *Eur. J. Inorg. Chem.*, 2008, 2186.
39 F. Rubio-Marcos, A. Del Campo, R. López-Juárez, J. J. Romero and J. F. Fernández, *J. Mater. Chem.*, 2012, **22**, 9714.
40 H. J. Trodahl, N. Klein, D. Damjanovic, N. Setter, B. Ludbrook, D. Rytz and M. Kuball, *Appl. Phys. Lett.*, 2008, **93**, 262901.
41 K. Kakimoto, K. Akao, Y. Guo and H. Ohsato, *Jpn. Journal J. Appl. Phys.*, 2005, **44**, 7064.
42 J. M. Jehng and I. E. Wachs, *Chem. Mater.*, 1991, **3**, 100
43 J.-J. Zhou, J.-F. Li and X.-W. Zhang, *J. Eur. Ceram. Soc.*, 2012, **32**, 267.
44 Z. X. Shen, Z. P. Hu, T. C. Chong, C. Y. Beh, S. H. Tang and M. H. Kuok, *Phys. Rev. B*, 1995, **52**, 3976.
45 Z. X. Shen, X. B. Wang, M. H. Kuok and S. H. Tang, *J. Raman Spectrosc.*, 1998, **29**, 379.
46 Y. Chang, Z. Yang, M. Dong, Z. Liu and Z. Wang, *Mater. Res. Bull.*, 2009, **44**, 538.
47 M. Kosec, B. Malič, A. Benčan and T. Rojac, *in Piezoelectric and Acoustic Materials for Transducer Applications*, ed. A. Safari and E. K. Akdoğan, Springer, New York, 2008, part. 2, ch. 5, pp. 81-82.
48 E. K. Akdogan, M. Allahverdi and A. Safari, *IEEE Trans. Ultrason. Eng.*, 2005, **52**, 746.
49 S. Zhang, H. J. Lee, C. Ma and X. Tan, *J. Am. Ceram. Soc.*, 2011, **94**, 3659.
50 J.-F. Li, K. Wang, F.-Y. Zhu, L.-Q. Cheng and F.-Z. Yao, *J. Am. Ceram. Soc.*, 2013. DOI: 10.1111/jace.12715.

